Effects of network structures on the fracture of hydrogel

Chenghai Li[a], Zhijian Wang[a], Yang Wang[b], Qiguang He[a], Rong Long[c], Shengqiang Cai[*ab]

[a] Department of Mechanical and Aerospace Engineering, University of California, San Diego, La Jolla, CA 92093, USA.

[b] Materials Science and Engineering Program, University of California, San Diego, La Jolla, CA 92093, USA

[c] Department of Mechanical Engineering, University of Colorado Boulder, Boulder, Colorado 80309, USA

Corresponding Author

*E-mail: shqcai@ucsd.edu

Abstract:

The polymer network structures and topologies in hydrogels can significantly affect their mechanical properties. The network structures can vary dramatically with different synthetic conditions of hydrogels. Herein, we study the effects of the polymer network structures on mechanical properties of poly(acrylamide) (PAAm) hydrogels synthesized through free radical polymerizations. We focus on investigating how the initial monomer concentration ϕ_0 during the synthesis influences the network structures and thus their mechanical properties. Specifically, we measure the swelling capability of the polymer network, the elasticity and fracture of swollen hydrogels with a fixed volume fraction of polymer. Our results have revealed that for PAAm hydrogels with the same volume fraction of polymer, their elasticity, stretchability, work of rupture and fracture toughness can vary significantly if ϕ_0 during the synthesis is different. Our study may provide important guideline for synthesizing hydrogels with tailorable mechanical properties without changing the chemistry and synthesis procedure.

Key words: Hydrogel; network structure and topology; inhomogeneity; elasticity; fracture; initial monomer concentration

1. Introduction

Hydrogel, a combination of water and crosslinked polymer network[1, 2], has been extensively explored in engineering applications including soft robots[3, 4], ionic electronics[5-7], tissue adhesives[8-10] and drug delivery[11] in recent years. Classical continuum theories for predicting the properties of hydrogels are often based on a simplified model assuming that the network is a perfect and homogenous three dimensional network[12, 13]. However, recent studies have demonstrated that the polymer network of hydrogels is highly inhomogeneous both spatially and locally (Figure 1), especially for those synthesized through free radical polymerizations[14-16]. The spatial inhomogeneity refers to the heterogeneous crosslinking, which often leads to coexistence of densely and loosely crosslinked regions with the distance on the order of magnitude of 10 ~ 100 nm[14-16]. Such distance can be also as large as the wavelength of visible light (~ several hundred nm), resulting in opaque hydrogels[14-17]. The local inhomogeneity includes dangling chains, loops, multiple crosslinking and trapped entanglements and other connectivity inhomogeneity (e.g., unreacted ends, double links, triple links and so on)[14-16, 18].

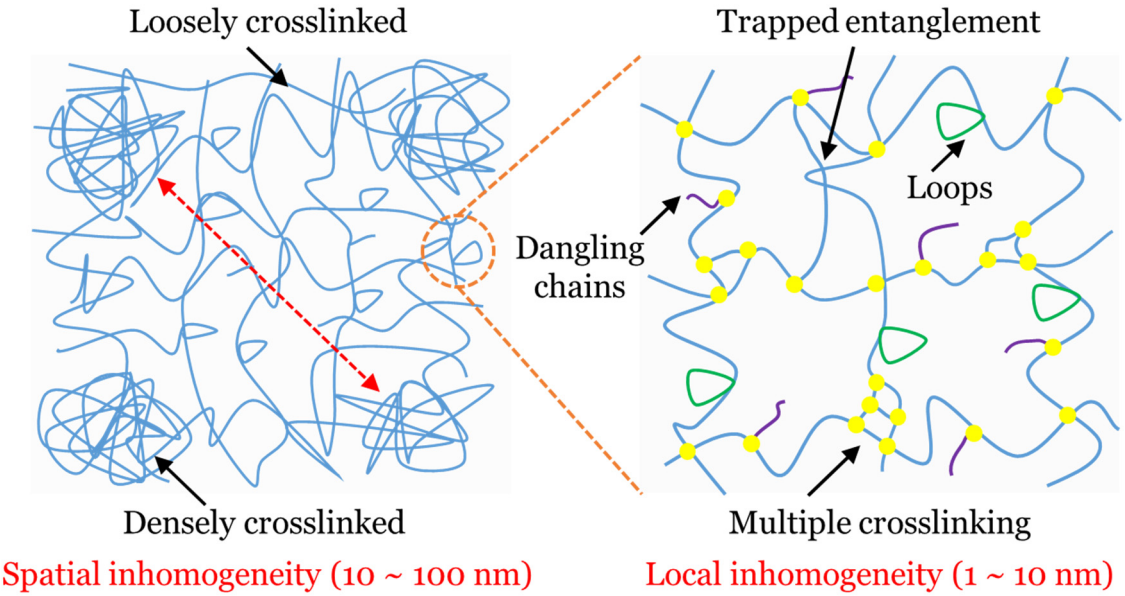

Figure 1. A real polymer network is inhomogeneous. For the polymers synthesized from free radical polymerizations, both spatial and local inhomogeneity can be often present in the network.

The spatial distance between densely and loosely crosslinked regions is typically on the order of magnitude of 10 ~ 100 nm. Local inhomogeneity includes dangling chains, loops, multiple crosslinking, trapped entanglements and other connectivity inhomogeneity (e.g., unreacted ends, double links, triple links and so on).

Many previous studies have revealed that network structures have significant impacts on the swelling[19], elasticity[20], fracture[21, 22], permeability[23] and optical properties[17] of hydrogels. A widely adopted model for understanding the effects of network structures is based on the concept of elastically effective chains[12, 13, 24]. When a polymer network is deformed, polymer chains attached to the network at only one end such as dangling chains cannot bear stress and thus don't contribute to the elasticity. Similarly, primary loops don't contribute to elasticity either. Elastically effective chains are those that deform and store elastic energy upon network deformation[24]. Elastically effective crosslinkings are those connecting at least two elastically effective chains. The density of effective chains, i.e. effective crosslinking density v_e, is often used to predict the elasticity of hydrogels, though a quantitative prediction of v_e itself is still challenging[12, 13, 24]. Some previous studies have further shown that in certain conditions, the number of elastically effective crosslinkings can be more than the total number of feeding crosslinker molecules because trapped entanglements may exist in the network[18, 25-28] (Figure 1), which behaves like additional effective crosslinkings.

For hydrogels synthesized from free radical polymerizations, the weight fraction of monomer denoted by ϕ_0 during the synthesis may vary greatly in experiments. Previous works have shown that tuning ϕ_0 during the synthesis can strongly affect the topology of the polymer network[25, 29] and thus the physical properties of synthesized hydrogels[17, 19, 29-33]. The relationship between ϕ_0 and the shear modulus and swelling capability of hydrogels has been intensively studied in the past[17, 19, 30-36]. In addition, a recent study by Yang et al showed that the inhomogeneous network structures could significantly affect the fracture of hydrogels synthesized

from free radical polymerizations[21]. However, according to our knowledge, there is no study on how ϕ_0 may affect the fracture of hydrogels.

In this article, we choose poly(acrylamide) (PAAm) hydrogels synthesized through free radical polymerizations as the model system. We focus on investigating how the initial monomer concentration ϕ_0 during the synthesis influences the network structures and thus their mechanical properties. Specifically, we measure the swelling capability of the polymer network, the elasticity and fracture of swollen hydrogels with a fixed volume fraction of polymer. Our results have shown that the effective crosslinking density increases with the increase of ϕ_0 and thus affect the swelling ratio and elasticity. Work of rupture and fracture toughness of the hydrogel decrease with the increase of ϕ_0 when the polymer fraction is fixed as same. Additionally, our current study also reveals a facile method to tailor toughness, work of rupture, strength and stretchability of a hydrogel by simply varying ϕ_0 during the synthesis. Our studies may shed some light on understanding the relationship between the microscopic structures of hydrogels and their macroscopic mechanical properties.

2. Experiments

2.1. Materials

All chemicals were used as purchased without any further purification. Acrylamide (AAm; Sigma-Aldrich 01700), N, N'-Methylenebis(acrylamide) (MBAA; Sigma-Aldrich M7279), Ammonium persulfate (APS; Sigma-Aldrich A3678), N,N,N',N'-Tetramethylethylenediamine (TEMED; Sigma-Aldrich T9281).

2.2. Synthesis of PAAm hydrogels with various ϕ_0

Solution (1) with 56 wt% monomer was prepared with 56 g AAm, 44 g deionized water and 0.034 g MBAA. Solution (2) was prepared with 10 g deionized water and 0.5705 g APS. The solutions were separately mixed using a stirrer until all chemicals were dissolved to get homogenous solutions. As shown in Figure 2, to synthesize hydrogels with various ϕ_0, the ratios

of both TEMED and solution (2) to solution (1) are kept as same. Firstly, every 1 g solution (1) (56 wt% AAm) was mixed with 20 μL solution (2) and 1.6 μL TEMED in a vial. Secondly, a given amount of deionized water was further added into the vial to dilute the initial monomer concentration ϕ_0 into various values from 14 wt% to 56 wt%. Then, the vial was sufficiently vibrated with a vortex mixer to get a homogeneous mixture. The synthesis procedures for ϕ_0 = 56 wt% and ϕ_0 = 14 wt% hydrogels are given as two examples. For hydrogel synthesized with ϕ_0 = 56 wt%, every 1 g solution (1) was mixed with 20 μL solution (2) and 1.6 μL TEMED. The mixture was poured into a glass mold with a 1 mm silicone spacer in the middle, and then cured in a 28 °C oven overnight. For hydrogel synthesized with ϕ_0 = 14 wt%, every 1 g solution (1) (56 wt% AAm) was firstly mixed with 20 μL solution (2) and 1.6 μL TEMED. 3 g deionized water was further added into the mixture to dilute the initial monomer concentration to 14 wt%. The molding and curing process are same as mentioned above.

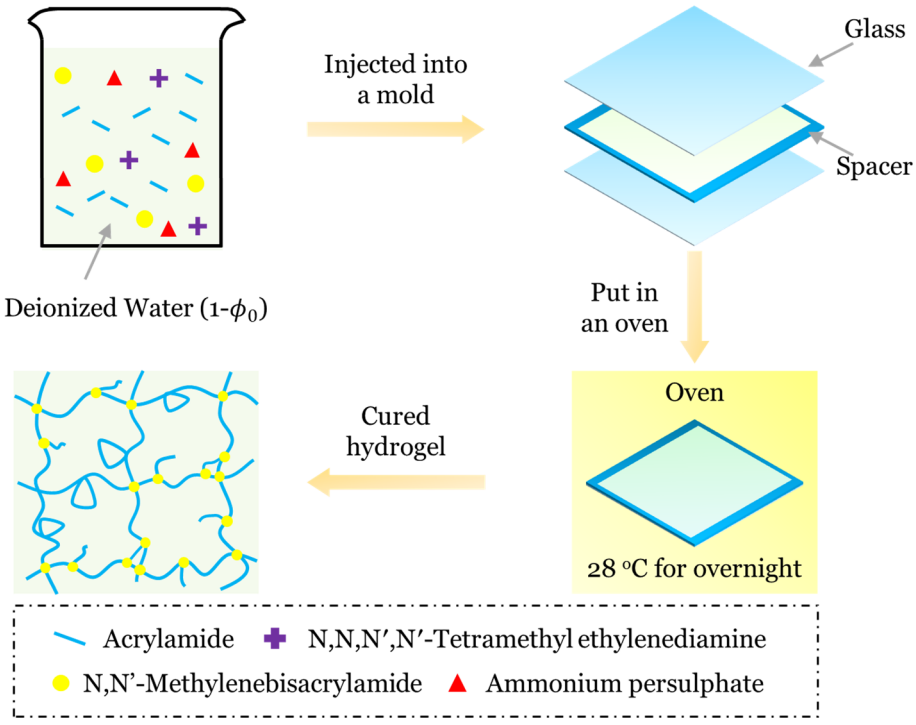

Figure 2. Steps to prepare PAAm hydrogels with various ϕ_0. AAm, MBAA, APS and TEMED with fixed molar ratios are mixed with a certain amount of water. The initial monomer concentration ϕ_0 is controlled by varying the initial weight fraction of water $(1 - \phi_0)$. The precursor is then

injected into a sandwiched glass mold with a 1 mm silicone spacer in the middle, and then left in a 28 °C oven for overnight to fully complete the free radical polymerization.

2.3. Free swelling and drying of hydrogels synthesized with various ϕ_0

As-prepared hydrogels were cut with a punch to get a disk with the diameter d = 12 mm and thickness t = 1 mm. The mass and the weight fraction of polymer for the disk are denoted by m_0 and ϕ_0, respectively. The mass of the feeding monomer is thus calculated as $m_{\text{feed}} = m_0 \times \phi_0$. The disk was immersed in deionized water for 3 days to achieve the equilibrium state with the mass denoted by m_{E}. The deionized water was changed every day to remove unreacted chemicals or possible free linear chains inside the hydrogel. We define the swelling ratio of the hydrogel as $SR = \frac{m_{\text{E}}}{m_{\text{feed}}} = \frac{m_{\text{E}}}{m_0 \times \phi_0}$. Then, the equilibrium hydrogel disk was put in an 85 °C oven for at least 24 hours to be totally dehydrated with the mass denoted by m_{dry}.

2.4. Controlled swelling of hydrogels to a fixed swelling ratio

As shown in Figure 3a, hydrogels synthesized with ϕ_0 = 14 wt% were directly used for all mechanical tests in current study. As shown in Figure 3b, hydrogels synthesized with ϕ_0 > 14 wt% were firstly swollen with a given amount of water to achieve a fixed polymer concentration ϕ_{f} = 14 wt%, and then used for all mechanical tests in current study. Taking hydrogels synthesized with ϕ_0 = 56 wt% as an example, we firstly measured the mass of the hydrogel m_0 and then sealed them in a plastic bag. Deionized water of $3m_0$ was poured into the bag. The hydrogel was swollen for at least 7 days to homogenize the distribution of water molecules. We also monitored the mass of the swollen hydrogel every day to guarantee that its overall mass achieved $4m_0$ before mechanical tests.

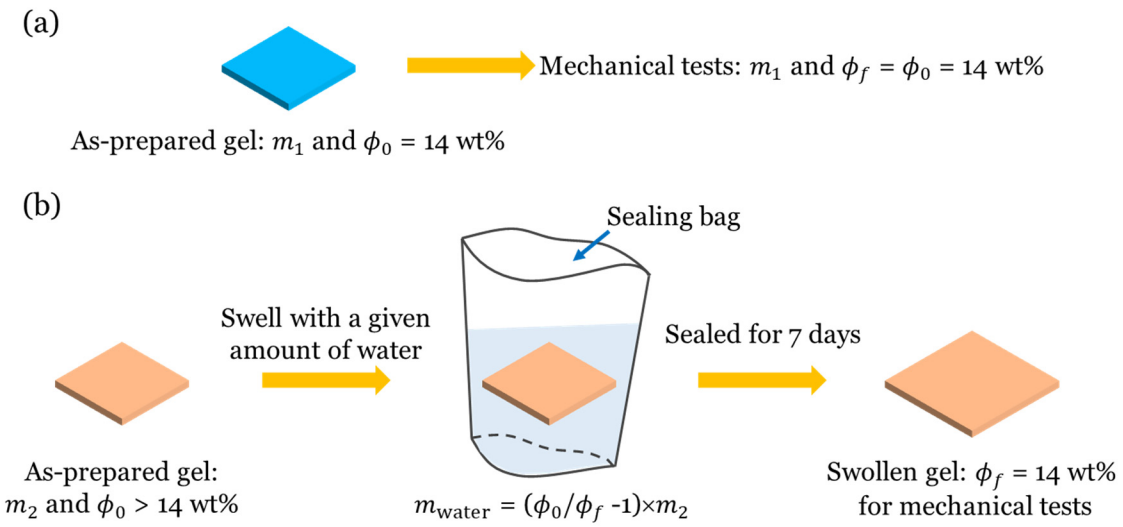

Figure 3. Controlled swelling of hydrogels synthesized with various ϕ_0 to a fixed weight fraction of polymer as 14 wt% for all mechanical tests. (a) As-prepared hydrogels with ϕ_0 = 14 wt% are directly used for mechanical tests. (b) As-prepared hydrogels with ϕ_0 > 14 wt% are first swollen in deionized water in a sealing a bag. The amount of the deionized water is carefully weighed to make sure in the final hydrogel, the weight fraction of the polymer network achieves 14 wt%. The gel is sealed in a plastic bag for at least 7 days to homogenize the distribution of water molecules inside the gel and then used for mechanical tests.

2.5. Characterizations of elasticity and fracture behavior of hydrogels with a fixed ϕ_f = 14 wt%

All the mechanical tests were performed with a tensile machine (5965 Dual Column Testing Systems; Instron) with 5000 N loading cell. Unless otherwise specified, in present study, all samples were loaded at a stretch rate of 0.5/s. Thus, in our experiments, the duration of the loading was within the range of 2 s ~ 60 s except for the stress relaxation test in Figure 9b. At this time scale, the effects of viscoelasticity and poroelasticity were both negligible[21, 37, 38]. The time scale of viscoelastic relaxation for PAAm is on the order of magnitude of 0.1 s ~ 1 s[37], much shorter than our experimental time scale. The length scale related to poroelasticity is the thickness of the hydrogel, t = 1 mm. The effective diffusivity of water molecule in PAAm is on the order of D ~

10^{-10} m^2/s[38] and thus the time necessary for poroelasticity to prevail is on the order of $t^2/D \sim 10^4$ s, which is much longer than our experimental time scale.

The height H = 10 mm and the width w = 60 mm in the undeformed state corresponds to the sample dimension parallel and perpendicular to the loading direction, respectively. The thickness t depends on the swelling process and was measured right before tests. Stretch λ is defined as the current height h divided by H in the loading direction. Nominal stress s is defined as the applied force divided by the cross-sectional area $t \times w$ in the reference state.

For characterizations of elasticity, unnotched samples were monotonously loaded until rupture. The shear modulus μ was calculated by the linear fitting of the slope of the nominal stress-stretch curve from λ = 1 to λ = 1.5. μ is one quarter of the slope for the pure shear test. Rupture stretch for unnotched samples was denoted as $\lambda_{\mathrm{rupture}}$. The work of rupture $W(\lambda_{\mathrm{rupture}})$ is calculated as $W(\lambda_{\mathrm{rupture}}) = \int_{\lambda=1}^{\lambda=\lambda_{\mathrm{rupture}}} s d\lambda$. The duration of the loading was shorter than 20 seconds and thus the dehydration of hydrogels during the test was negligible.

For characterizations of fracture, notched samples with an initial cut of C_0 = 15 mm at the middle of the height were monotonously loaded until fracture. The critical stretch where the crack started to propagate was denoted as λ_{c}. The toughness Γ was calculated by firstly integrating the nominal stress-stretch curve of the unnotched sample from λ = 1 to $\lambda = \lambda_{\mathrm{c}}$ get $W(\lambda_{\mathrm{c}})$, and then multiplied by H, i.e., $\Gamma = H \times W(\lambda_{\mathrm{c}})$. The duration of the loading was shorter than 12 seconds and thus the dehydration of hydrogels during the test was also negligible.

2.6. Hysteresis measurements for hydrogels with a fixed ϕ_{f} = 14 wt%

For the hysteresis measurements, unnotched samples were cyclically loaded to various given maximal stretches λ_{max}. The nominal stress-stretch curves under various λ_{max} were recorded in different figures.

2.7. Rate-dependence and stress relaxation of hydrogels

To further check the viscoelasticity, we used hydrogels synthesized at ϕ_0 = 56 wt% but a fixed polymer fraction as 14 wt%. Unnotched samples were monotonically loaded with two different strain rates of 0.5/s and 0.02/s respectively until rupture under pure shear test. Stress relaxation test was separately conducted under pure shear test: the unnotched sample was stretched to λ = 2 with a strain rate of 0.5/s and then we kept the stretch for a long time ~ 1800 s to monitor the change of nominal stress. During the stress relaxation test, we tried to keep the hydrogel sample in a fully hydrated environment as follows: a homemade chamber was used to establish a relatively enclosed environment. Then, a humidifier was used to generate enough water vapor, which was guided into the chamber through a tube. We measured the mass of the sample before and after the relaxation test. The increase of the hydrogel sample was ~1.50 wt%, which is assumed to have negligible effect on the result.

3. Results

3.1. Effects of ϕ_0 on free swelling and effective crosslinking density of hydrogels

As mentioned in Figure 2, we synthesized PAAm hydrogels with various ϕ_0 while keeping the ratios of MBAA, APS and TEMED to AAm as constants. Like most hydrogels synthesized through free radical polymerization, the gelation process of PAAm hydrogel includes two main sequential stages: initial intra-microgel chain growth and later inter-microgel connection[29, 39-44]. Since the rate of crosslinking is often statistically larger than that of chain propagation in the first stage and thus many separated microgels are formed. In the second stage, when the concentration of the crosslinker decreases, the remaining monomers start to react with microgels, which grow in size and get connected with each other. Therefore, microgels aggregate into a macrogel. During this process, intra-microgel chain growth and inter-microgel connection compete, which can be influenced by the concentrations of monomer, crosslinker, and microgels. Cyclization and multiple crosslinking have been confirmed to happen during the gelation process[19, 30, 45]. Cyclization leads to the formation of loops and primary loops cannot bear stress and thus reduces

v_e. Multiple crosslinking consumes crosslinkers in the first stage and thus the later formed polymer chains in the second stage have a much longer chain length[29, 40-42]. A large fraction of crosslinkers form ineffective crosslinking in the multiple crosslinking process, which also reduces v_e. Previous works have shown that cyclization and multiple crosslinking are more probable at a lower ϕ_0 during the gelation[19, 30, 45], which results in the decrease of v_e. Moreover, it has been shown that, with the decrease of ϕ_0, less trapped entanglements may form in the polymer network, which can also decrease v_e[25, 27, 28].

Herein, we first study the free swelling of PAAm hydrogels synthesized with different ϕ_0. For convenience, we define the swelling ratio as $SR = \frac{m_E}{m_{feed}} = \frac{m_E}{m_0 \times \phi_0}$, where m_E is the mass of a swollen gel in the equilibrium state, m_{feed} is the mass of the feeding monomer, and m_0 is the mass of the as-prepared gel. SR describes the water adsorption capacity of a polymer network. We fully swell as-prepared hydrogels in deionized water for at least 3 days and the deionized water is changed every day to remove unreacted chemicals or possible free linear chains inside the hydrogels. Then, we measure the mass of the swollen gels in equilibrium state, and finally completely dry the gel at 85 °C to measure the mass of dry polymer denoted by m_{dry} (Figure 4a). The ratios of m_{dry} to m_{feed} are close to 100% for hydrogels synthesized with various ϕ_0 (Figure 4b). We note that the ratio is slightly above 100% (Figure 4b), which can be attributed to the residual bound water inside the polymer network[46]. For simplicity, we neglect the slight difference between m_{dry} and m_{feed}, and use m_{feed} to define ϕ_0 in this article. We found that SR of a dry polymer network at the equilibrium state decreases with the increase of ϕ_0 (Figure 4c), which is consistent with previous studies[17, 19, 29, 30, 32, 33]. By using the concept of v_e, several quantitative models relating SR and ϕ_0 have been developed[25, 32, 47-50]. It is noted that the theoretical predictions of the elastic properties of hydrogels synthesized with various ϕ_0 still have noticeable deviations from experiments[32, 50].

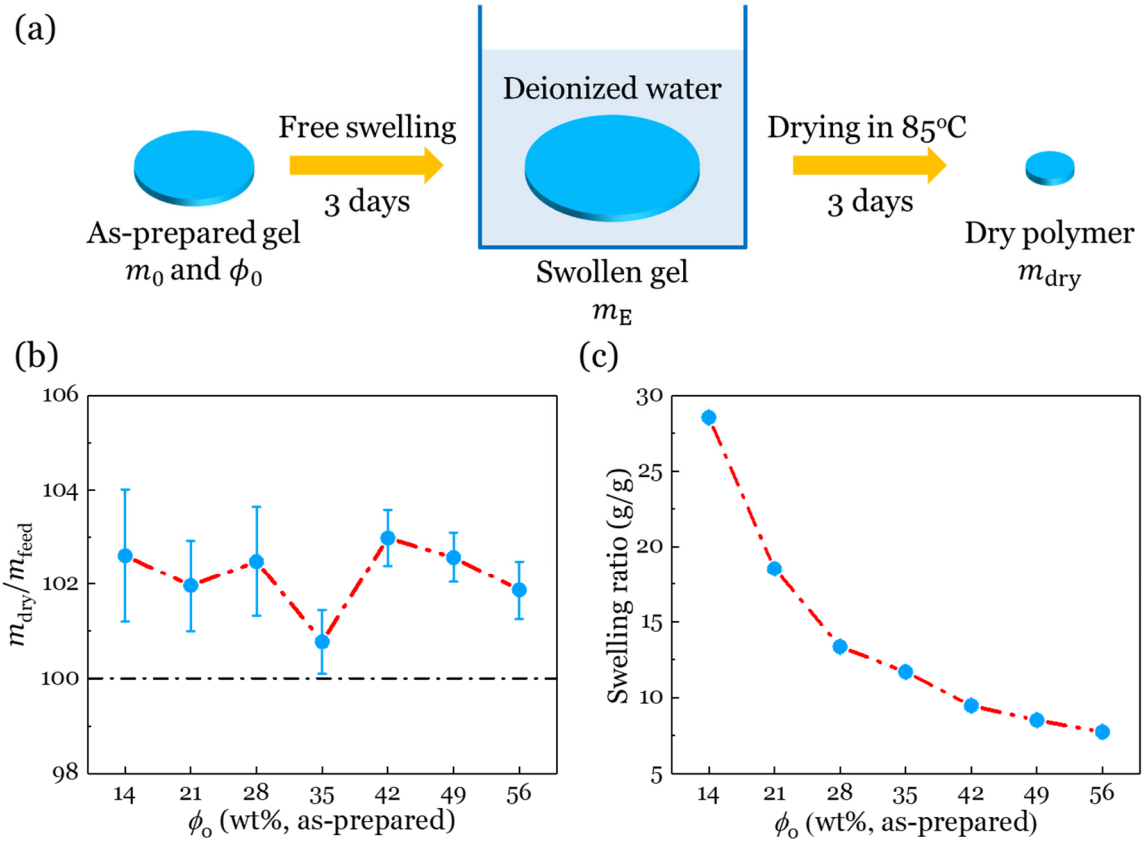

Figure 4. Free swelling and drying experiments of PAAm gels synthesized at various ϕ_0. (a) As-prepared hydrogel disk with mass denoted by m_0 and weight fraction of the polymer denoted by ϕ_0 is swollen in deionized water for 3 days to achieve equilibrium state with mass denoted by m_E. Then, the hydrogel is put in an 85 °C oven for 3 days to be totally dehydrated with the mass denoted by m_{dry}. (b) The ratios of the mass of the dry polymer m_{dry} to the mass of the feeding monomer as $m_{feed} = m_0 \times \phi_0$ are close to 100% for hydrogels synthesized at various ϕ_0, indicating that nearly all monomers were converted to polymer network independent of ϕ_0. (c) The swelling ratio of dry polymers at equilibrium states decreases with the increase of ϕ_0.

3.2. Effects of ϕ_0 on the mechanical properties of unnotched hydrogels with a fixed ϕ_f = 14 wt%

For all the following mechanical measurements, we fix the weight fraction of polymer in hydrogels to 14 wt%, which corresponds to a volume fraction as ϕ_V = 12.8%. As mentioned in the

experiments section, hydrogels synthesized with ϕ_0 = 14 wt% were directly used for measurements (Figure 3a). Hydrogels synthesized with ϕ_0 > 14 wt% are first swollen to reach the targeted weight fraction 14 wt% and then equilibrated in a sealing bag, after which measurements were performed (Figure 3b). Unless otherwise specified, we used a strain rate as 0.5/s for all the following measurements, which was chosen to minimize the influence of viscoelasticity and poroelasticity[21, 37, 38].

We first conduct pure shear tests on hydrogel of rectangular shape with the aspect ratio of 6. Figure 5a shows the corresponding nominal stress-stretch curves. For a incompressible Neo-Hookean model, the shear modulus μ is one quarter of the initial slope of the s-λ curve under pure shear tests[21]. We found that within the range of ϕ_0 in this study, μ can vary as large as 10 times (Figure 5b). The increase of μ with the increase of ϕ_0 is consistent with previous studies[17, 19, 28, 30, 32, 33, 50]. As mentioned before, a quantitative prediction of v_e from the synthesis condition is still challenging[12, 13, 24]. Thus, we determine v_e through the experimental μ following a previous study[51]: we assume the network strands can be considered as Gaussian chains and swelling introduces an affine volumetric stretch to the network, which results in the following relation between v_e and μ as $\mu = {\phi_V}^{1/3}\left(\frac{\beta\phi_0}{1-\phi_0+\beta\phi_0}\right)^{2/3} v_e RT$, where β is ratio of the density of water to the density of dry polymer, R and T take their usual meanings. Furthermore, v_e is determined by the effective number of monomers in each polymer chain n with $v_e = \frac{1}{nVN_A}$, where V is the volume of a monomer and N_A is the Avogadro's number. Thus, we can compute n from μ through v_e. Figure 5b shows that n decreases with the increase of ϕ_0, which is attributed to two reasons. First, at a larger ϕ_0, the formations of elastically ineffective chains are less probable during the synthesis, resulting in a larger v_e and thus a smaller n. Second, previous studies have shown that at a larger ϕ_0, the formation of trapped entanglements is more probable[25, 27, 28], which can also increase v_e and thus a smaller n.

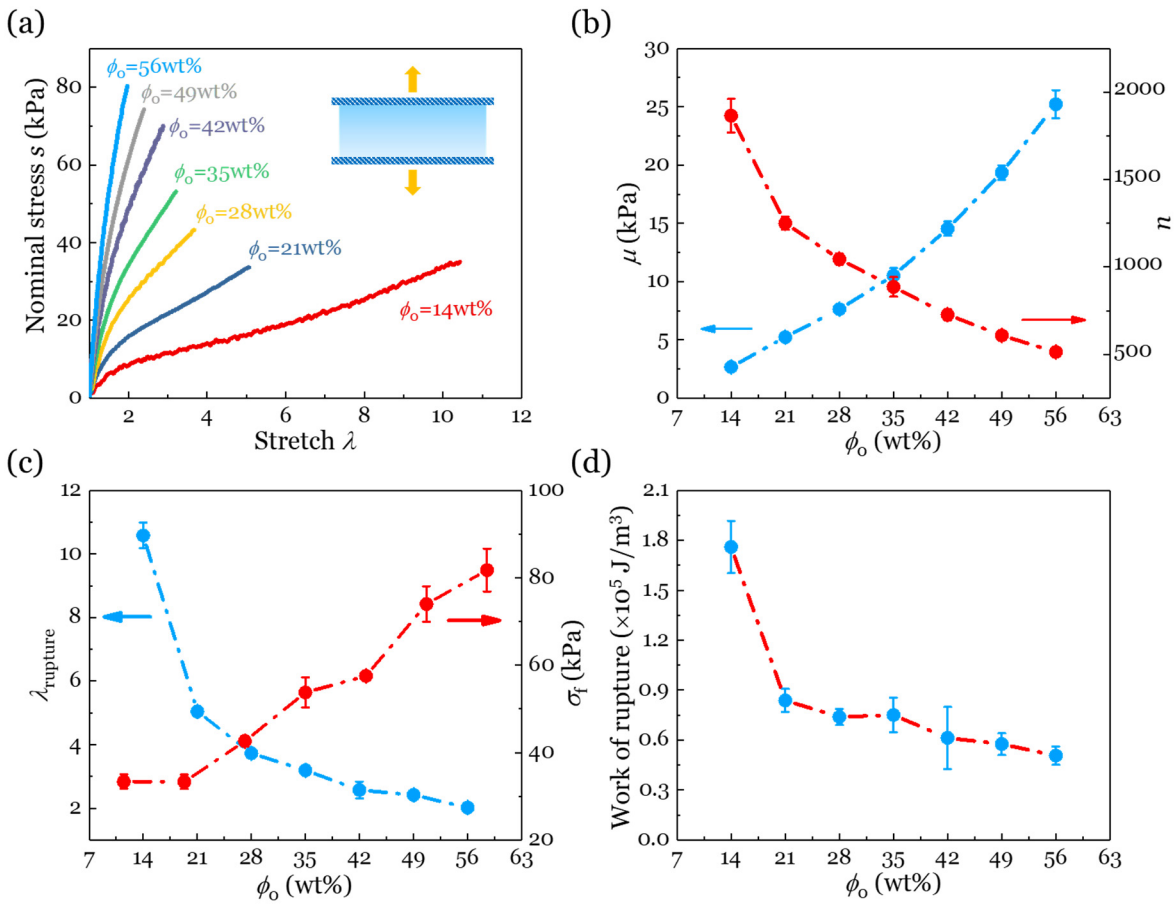

Figure 5. Mechanical properties of hydrogels synthesized at various ϕ_0 but with a fixed weight fraction of polymer as 14 wt%. (a) Nominal stress-stretch curves of unnotched hydrogels under pure shear tests. (b) The shear modulus μ increases with the increase of ϕ_0 but the effective chain length n decreases with the increase of ϕ_0. (c) The rupture stretch λ_{rupture} decreases with the increases of ϕ_0, while the strength σ_{f} increases with the increases of ϕ_0. (d) The work of rupture of the hydrogels decreases significantly with the increase of ϕ_0.

We further plot the rupture stretch λ_{rupture} and strength σ_{f} of the hydrogel (Figure 5c) and find that the hydrogel synthesized with a lower ϕ_0 has a larger λ_{rupture} but smaller σ_{f}. Such trends can be partially understood by the fact that ν_{e} is smaller for hydrogels synthesized at lower ϕ_0. We further calculate the work of rupture as $W(\lambda_{\text{rupture}}) = \int_{\lambda=1}^{\lambda=\lambda_{\text{rupture}}} s d\lambda$. Figure 5d shows that

$W(\lambda_{\text{rupture}})$ decreases with the increase of ϕ_0. These results have clearly shown that the network structures have significant impact on the fracture of hydrogels. We postulate that for the hydrogel synthesized with a lower ϕ_0, greater spatial inhomogeneity can be present in the network and more significant bulk damage occurs during its deformation, which leads to a larger $W(\lambda_{\text{rupture}})$. Detailed models for relating the network structures to λ_{rupture}, σ_{f} and $W(\lambda_{\text{rupture}})$ require a separate study.

3.3. Effects of ϕ_0 on mechanical properties of notched hydrogels with a fixed ϕ_{f} = 14 wt%

To systematically investigate the fracture, we next conduct pure shear tests on hydrogel samples with a precut. Notched samples are monotonically loaded until fracture. The critical stretch λ_{c} where the crack starts to propagate is measured. Fracture toughness Γ is calculated by integrating the s-λ curve of the unnotched sample from $\lambda = 1$ to $\lambda = \lambda_{\text{c}}$ to get $W(\lambda_{\text{c}})$, and then multiplied by the sample height H in the undeformed state[1, 52], i.e., $\Gamma = H \times W(\lambda_{\text{c}})$ (Figure 6a). We plot the s-λ curves of notched samples in Figure 6b. Our results show that λ_{c} decreases significantly with the increase of ϕ_0 as shown in Figure 6c. We found that Γ decreases significantly when ϕ_0 is increased from 14 wt% to 28 wt%, and nearly reaches a constant when ϕ_0 is between 28 wt% and 35 wt%, and then decreases again when ϕ_0 is increased from 35 wt% to 56 wt% (Figure 6d). Γ is 650.86 ± 86.00 J/m² for hydrogels with ϕ_0 = 14 wt% but reduced to 223.69 ± 29.96 J/m² for hydrogels with ϕ_0 = 56 wt%.

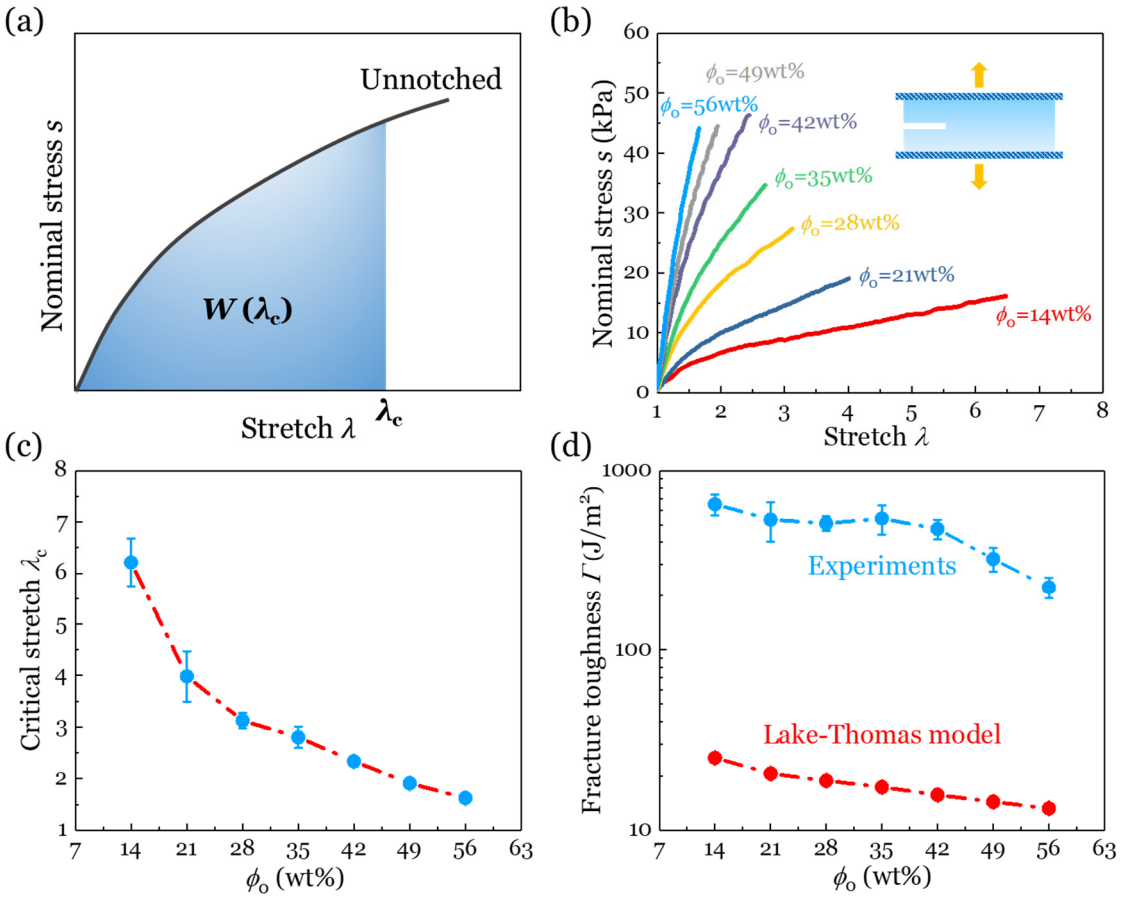

Figure 6. Fracture of notched hydrogels under pure shear tests with a fixed weight fraction of polymer as 14 wt%. (a) Calculation of fracture toughness of the gels under pure shear tests. Critical stretch is λ_c determined from pure shear test of the notched samples. Integration of the stress-stretch curve of the unnotched sample from $\lambda = 1$ to $\lambda = \lambda_c$ gives $W(\lambda_c)$. Fracture toughness is calculated as $\Gamma = H \times W(\lambda_c)$, where H is the sample height in the undeformed state. (b) The nominal stress-stretch curves of notched samples. (c) The critical stretch λ_c of the hydrogels decreases with the increase of ϕ_0. (d) The experimental fracture toughness of the hydrogel decreases significantly with the increase of ϕ_0. The predicted fracture toughness from Lake-Thomas model using the chain length n in Figure 5b decreases with the increase of the ϕ_0.

Previous studies have shown that Lake-Thomas model greatly underestimated the fracture toughness of PAAm hydrogels[21, 22]. Based on the Lake-Thomas picture[53], the fracture toughness can be estimated as: $\Gamma_0 = {\phi_V}^{2/3}\sqrt{n}aJ/V$, where a is the length of a monomer, J is the bond energy of a covalent bond and V is the volume of a monomer. Considering the ideal network and with the same parameters as previous reports[21] and using the range of n found in Figure 5b, the Lake-Thomas predictions ranges from Γ_0 = 25.2 ± 0.6 J/m² to 13.2 ± 0.3 J/m² with the increase of ϕ_0 (Figure 6d). It has been postulated that the deviation of the experimental fracture toughness from the theoretical prediction of PAAm hydrogels is closely associated with inhomogeneous network structures[21]. However, previous works did not study how ϕ_0 could affect the network structures and topologies of hydrogels and thus their fracture properties[21], which is an important parameter for hydrogel synthesis.

It is noted that many previous studies have used scattering experiments to detect the inhomogeneity of hydrogel networks and shown that the free radical polymerized hydrogel networks become more homogeneous with the increase of ϕ_0 in certain conditions[14-17, 19, 27, 30, 36, 54, 55]. Herein, our results have further revealed that with the increase of ϕ_0 during the synthesis, the fracture toughness of hydrogels decreases, which can be attributed to a more homogenously crosslinked network structure of hydrogels and a smaller number of defects with the increase of ϕ_0. Such trend is similar with the work of rupture as shown in Figure 5d. Crack tip deformation in the hydrogels just before the onset of crack propagation is shown in Figure 7. We found that when the weight fraction of polymer is fixed as 14 wt%, crack blunting is more significant for hydrogels synthesized with a low ϕ_0 but becomes less significant for hydrogels synthesized with a higher ϕ_0. Such experimental observations have confirmed the change of network structures with the change of ϕ_0.

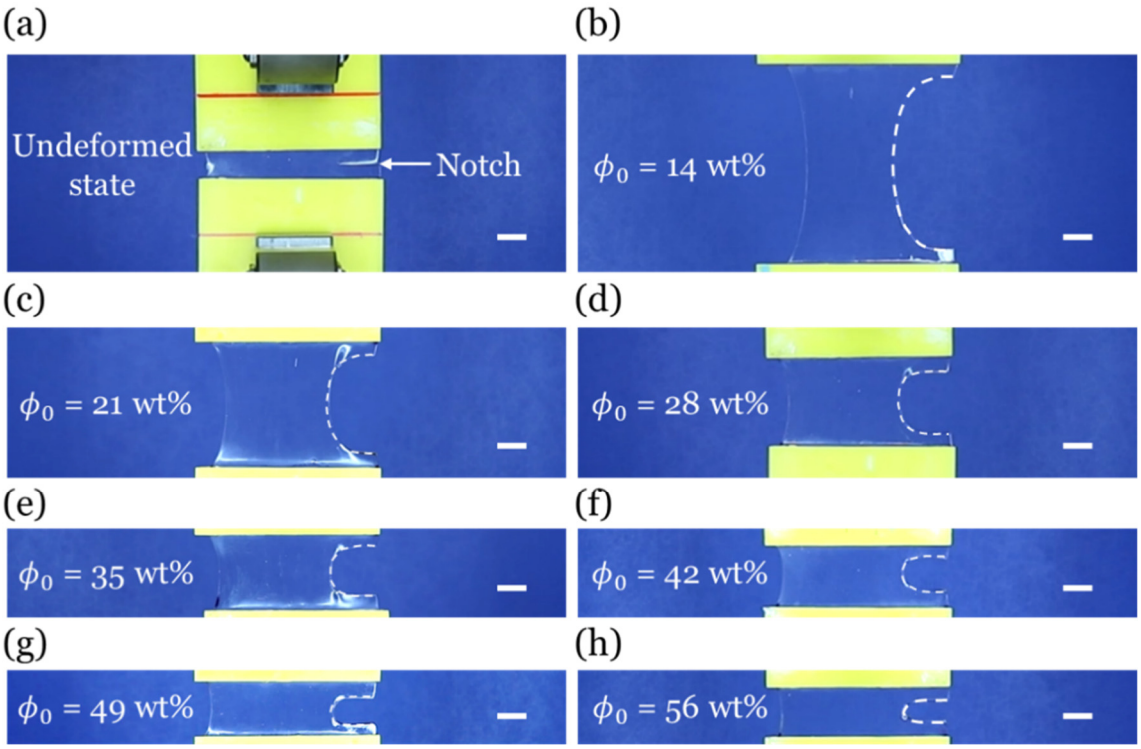

Figure 7. Crack tip deformation for notched hydrogels synthesized at various ϕ_0 but a fixed weight fraction of polymer as 14 wt% just before the onset of crack propagation. (a) Undeformed state of the notched hydrogel. The deformed state of notched hydrogels just before the crack extension when ϕ_0 is (b) 14 wt%, (c) 21 wt%, (d) 28 wt%, (e) 35 wt%, (f) 42 wt%, (g) 49 wt% and (h) 56 wt%, respectively. Crack blunting is more significant for hydrogels synthesized with a low ϕ_0 but becomes less significant for hydrogels synthesized with a high ϕ_0. The scale bars are all 1cm.

3.4. Effects of ϕ_0 on viscoelasticity of unnotched hydrogels with a fixed ϕ_f = 14 wt%

It has been known that inelastic dissipation such as the viscosity inside the material during the deformation can contribute to its fracture toughness[1, 2, 56, 57]. To examine if the difference of the fracture toughness originates from the different inelastic dissipation inside hydrogels, we next conduct the loading-unloading tests of hydrogels synthesized with various ϕ_0. Since λ_{rupture} depends on ϕ_0 for unnotched hydrogels (Figure 5c), we conduct loading-unloading tests to

various maximal stretches λ_{max} and plot them in different figures (see Figure 8). The ratio of the area between loading and unloading curve to the whole area under loading curve is a quantitative description of the viscoelastic dissipation during the deformation of a material[58]. Results show that the hysteresis of hydrogels with various ϕ_0 are always small at various stretch levels. We further compared the nominal stress-stretch curves for hydrogels synthesized with ϕ_0 = 56 wt% but a fixed ϕ_f = 14 wt% under two different strain rates and found negligible difference, indicating that the hydrogels used in the current study are nearly rate-independent (Figure 9a). We also performed stress relaxation tests and found negligible relaxation over a long time ~ 1800s (Figure 9b), indicating that the hydrogels in this study are nearly purely elastic. Thus, we conclude that the viscoelasticity has minimal effect on the results in the current study.

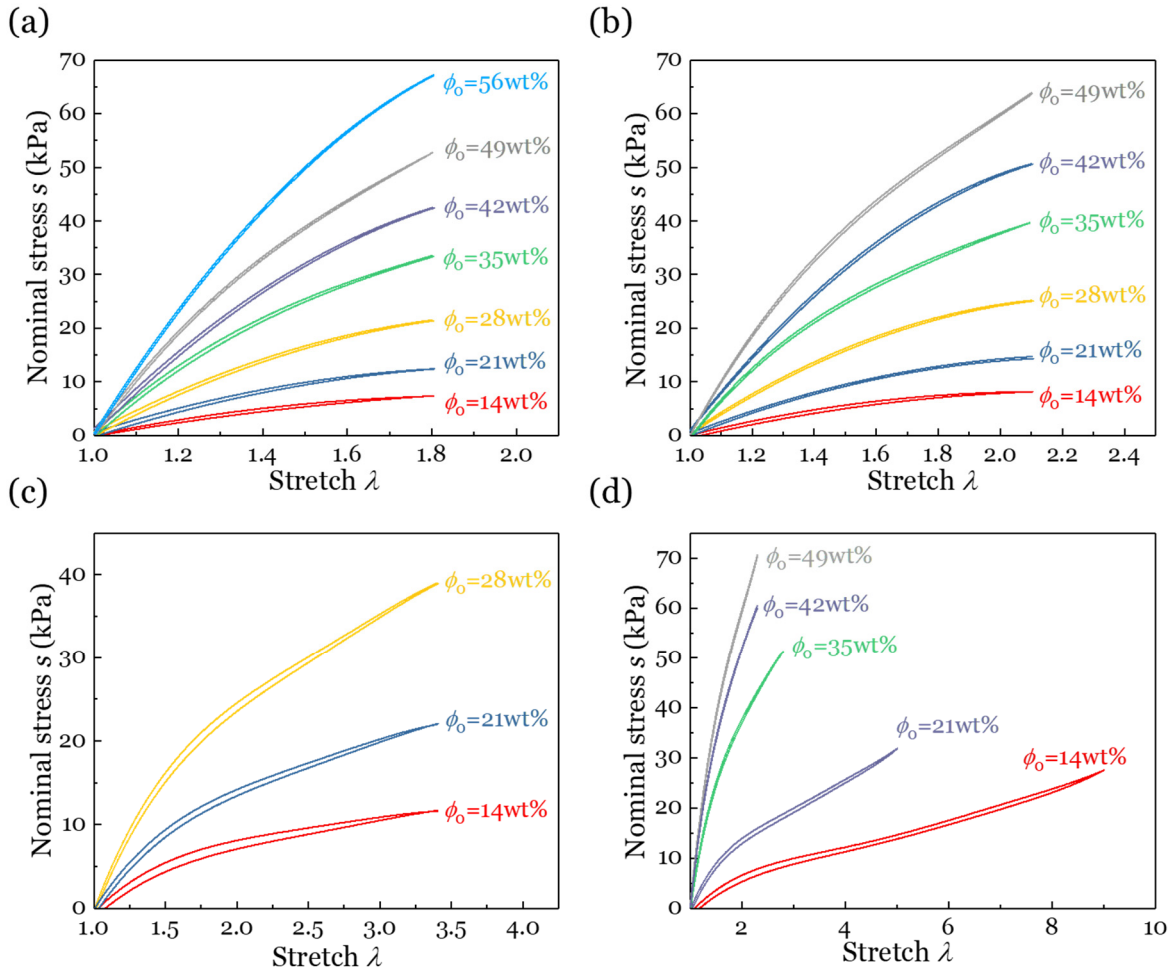

Figure 8. Hysteresis of hydrogels synthesized at various ϕ_0 but with a fixed weight fraction of polymer as 14 wt% under pure shear tests. Since $\lambda_{rupture}$ depends on ϕ_0 during the gel synthesis, we conduct loading and unloading tests to various maximal stretches: (a) λ_{max} = 1.8 (b) λ_{max} = 2.1, (c) λ_{max} = 3.4, and (d) λ_{max} = 2.3 for hydrogels synthesized with ϕ_0 = 49 wt% and 42 wt%, λ_{max} = 2.8 for hydrogels synthesized with ϕ_0 = 35 wt%, λ_{max} = 5 for hydrogels synthesized with ϕ_0 = 21 wt% and λ_{max} = 9 for hydrogels synthesized with ϕ_0 = 14 wt%, respectively.

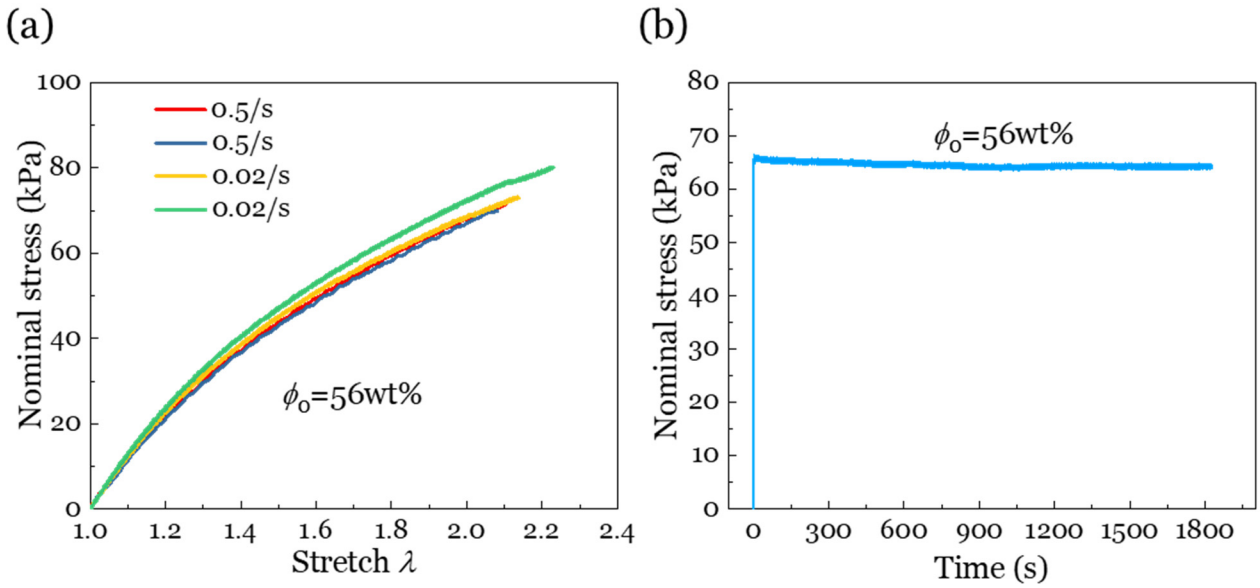

Figure 9. Experiments to check the viscoelasticity of hydrogels synthesized at ϕ_0 = 56 wt% but a fixed fraction of polymer as 14 wt%. (a) Nominal stress-stretch curves of unnotched hydrogel samples under pure shear tests using two different strain rates. (b) Stress relaxation test of the unnotched hydrogel sample under pure shear test. The sample was stretched to λ = 2 with a strain rate of 0.5/s and then we maintain the stretch unchanged. The stress shows negligible decrease over a long time ~ 1800 s.

3.5. Effects of ϕ_0 on the two fracture-related length scales of hydrogels with a fixed ϕ_f = 14 wt%

At last, we experimentally determine two important length scales related to the fracture of stretchable materials[59]. One is the elasto-cohesive length scale denoted by l and the other is fracto-cohesive length scale denoted by ξ. It is noted that both l and ξ are defined at reference state (Figure 10a). The notched sample in the deformed state and the two length scales are also illustrated in Figure 10b. The length scale $l = \Gamma/E$ defines a size of a zone near the crack tip (Figure 10a). K-field obtained from linear fracture mechanics is not valid anymore inside the zone, where finite deformation needs to be considered. Figure 10c shows that the elasto-cohesive length l of the hydrogel decreases with the increase of ϕ_0. As discussed in the previous study[59], the length scale l scales with the crack tip opening displacement before the crack starts to propagate. Large elasto-cohesive length leads to more significant crack blunting, which is confirmed by the crack tip deformation before fracture (Figure 7).

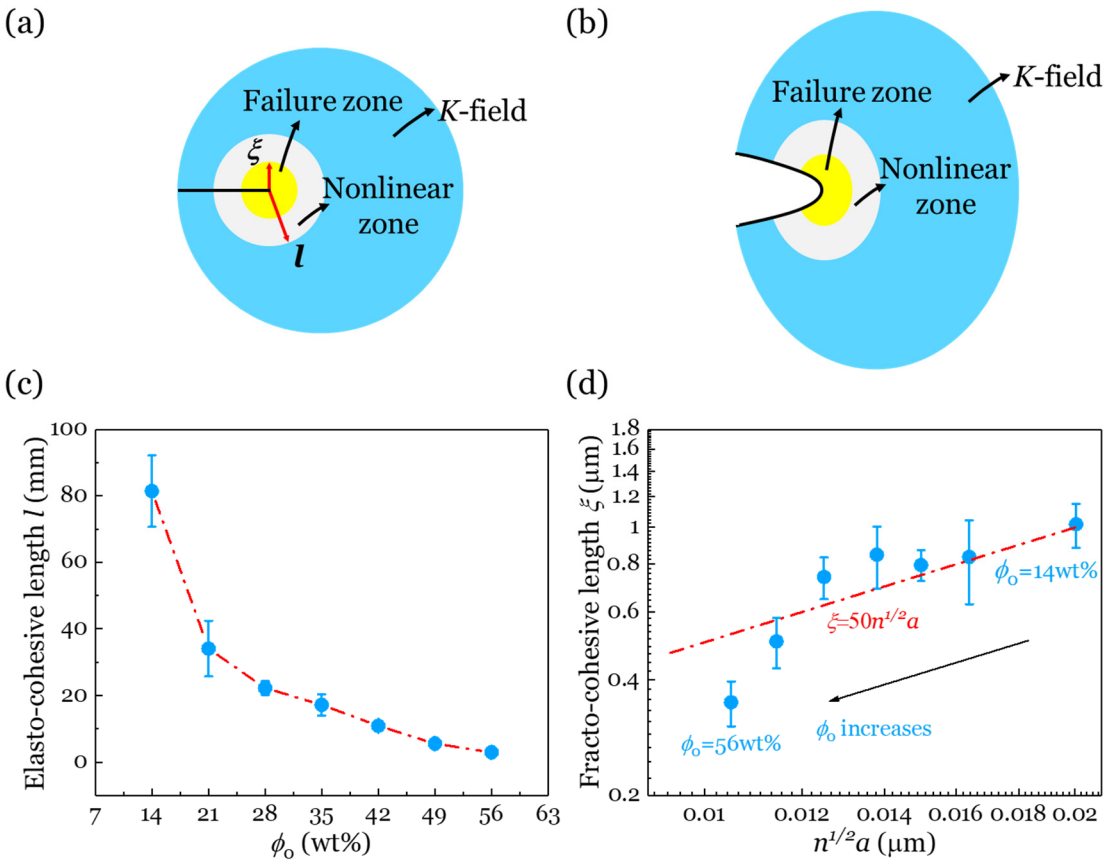

Figure 10. Two fracture-related length scales of the PAAm gel synthesized at various ϕ_0 but a fixed weight fraction of polymer as 14 wt%. (a) The elasto-cohesive length scale l represents the size of an area near the crack tip where nonlinear elasticity becomes important. The fracto-cohesive length scale ξ describes the size of the damage processing zone near a crack tip. Both l and ξ are defined in the reference state. (b) The notched sample in the deformed state. (c) The elasto-cohesive length scale l decreases with the increase of ϕ_0. (d) The fracto-cohesive length scale ξ increases with the increase of the ideal mesh size $n^{1/2}a$. We plot the dash dot line $\xi = 50n^{1/2}a$ together with the experimental measurements. Within the range of ϕ_0 in present study, ξ is nearly 50 times of $n^{1/2}a$, which indicates the much more amplified dissipation zone size compared to the ideal mesh size.

The length scale $\xi = \Gamma/W_{\text{th}}$ is a measurement of the fracture processing zone size[21, 59] where W_{th} is the theoretical work of rupture calculated as $W_{th} = \phi_{\text{V}}J/V \sim 6.4 \times 10^8\ \text{J/m}^3$. The length scale ξ also scales the size of the flaw sensitivity[21, 60]. For a perfect network with the same chain length, the Lake-Thomas model predicts that the fracto-cohesive length scale is $\xi = \Gamma_0/W_{\text{th}} = \left(\frac{\phi_{\text{V}}^{\frac{2}{3}}\sqrt{n}aJ}{V}\right) / \left(\frac{\phi_{\text{V}}J}{V}\right) = {\phi_{\text{V}}}^{-1/3}\sqrt{n}a$, which indicates that the fracture processing zone size near the crack tip during fracture scales with the mesh size $\sqrt{n}a$. For our inhomogeneous PAAm hydrogels, we calculated the fracto-cohesive length scale ξ using the experimentally measured Γ from Figure 6d and the theoretical work of ruptureW_{th}, which characterizes how much the PAAm network is deviated from the perfect network. The ξ versus the ideal mesh size calculated as $n^{1/2}a$ is shown in Figure 10d. We found that ξ decreases with the increase of ϕ_0. ξ is much larger than the ideal mesh size $n^{1/2}a$, which is around 50 times as shown with the red dash dot curve, indicating the much more amplified fracture processing zone size than the mesh size during fracture. In contrast, for ideal hydrogels synthesized from PEG, ξ is almost on the same order of

magnitude of $n^{1/2}a$, which is consistent with Lake-Thomas model[59, 61]. The fracto-cohesive length scale is on the same order of magnitude of the length scale of the inhomogeneity in the PAAm gel as reported before[14-16].

4. Discussions

Finally, with current understandings of the molecular structures of the PAAm hydrogels synthesized with various ϕ_0 and experimental results, we try to tentatively explain the influence of ϕ_0 on the hydrogel fracture. Recall that fracture toughness can be often decomposed to two parts: $\Gamma = \Gamma_0 + \Gamma_D$, where Γ_D is the toughness contributed from bulk dissipation and Γ_0 is the intrinsic toughness: (1) For hydrogel with lower ϕ_0, the effective crosslinking density v_e is smaller, corresponding to a longer effective elastic chain length (i.e., larger n) and thus a higher Γ_0[21, 53]. (2) The interconnected loosely and densely crosslinked regions in hydrogels form a composite-like structure. Recent studies have shown that fracture toughness of such composite can be enhanced due to stress deconcentration at the interface and thus a higher energy release rate is needed to break the hard domains to advance the crack[27, 58, 62, 63]. Such spatial inhomogeneity becomes less significant at a high ϕ_0 and thus such toughening effect is reduced. (3) At a lower ϕ_0, the space between microgels are much larger, which may behave as small voids to toughen the material[64]. (4) Crack blunting is considered to be an important toughening mechanism for soft solids[59], which becomes less significant with the increase of ϕ_0. (5) Heterogeneous chain lengths of polymer network may also increase fracture toughness[21, 65]. Before a long polymer chain at the crack front breaks, the network transmits the high stress from the crack front to the network. In the network, some short chains away from the fracture plane may break first while long chains remain intact. Consequently, to advance the crack, not only a layer of polymer chains on the crack plane is ruptured, but also additional short chains away from the crack plane needs to be broken. At a higher ϕ_0, the polymer network in the gel have more uniformly distributed chain length and thus lower fracture toughness.

5. Conclusions

In conclusion, real polymer networks of hydrogels are inhomogeneous. Depending on the value of ϕ_0, the network structures and topologies can vary significantly. Our results have shown that the effective crosslinking density increases with the increase of ϕ_0 and thus affect the swelling ratio and elasticity. Work of rupture and fracture toughness of the hydrogel decrease with the increase of ϕ_0 when the polymer fraction is fixed. More efforts will be required to quantitatively understand the effects of ϕ_0 on the hydrogel fracture, which may enable precise controls of the stretchability, strength and flaw-sensitivity of hydrogels. Additionally, our current study also reveals a facile method to tailor toughness, work of rupture, strength and stretchability of a hydrogel by simply varying ϕ_0 during the synthesis. We hope this study will provide useful insights into the design of hydrogels and promote their applications.

Declaration of Competing Interest

The authors declare that they have no known competing financial interests or personal relationships that could have appeared to influence the work reported in this paper.

Acknowledgments

S.C. acknowledges supported from ONR with the grant number: N00014-17-1-2056. R.L. acknowledges support from the National Science Foundation through a CAREER award (NSF CMMI-1752449).

Reference

1. Sun, J.-Y.; Zhao, X.; Illeperuma, W. R.; Chaudhuri, O.; Oh, K. H.; Mooney, D. J.; Vlassak, J. J.; Suo, Z., Highly stretchable and tough hydrogels. *Nature* **2012,** *489* (7414), 133-136.
2. Gong, J. P.; Katsuyama, Y.; Kurokawa, T.; Osada, Y., Double‐network hydrogels with extremely high mechanical strength. *Advanced materials* **2003,** *15* (14), 1155-1158.

3. Yang, H.; Li, C.; Yang, M.; Pan, Y.; Yin, Q.; Tang, J.; Qi, H. J.; Suo, Z., Printing hydrogels and elastomers in arbitrary sequence with strong adhesion. *Advanced Functional Materials* **2019,** *29* (27), 1901721.
4. Banerjee, H.; Suhail, M.; Ren, H., Hydrogel actuators and sensors for biomedical soft robots: brief overview with impending challenges. *Biomimetics* **2018,** *3* (3), 15.
5. Yuk, H.; Lu, B.; Zhao, X., Hydrogel bioelectronics. *Chemical Society Reviews* **2019,** *48* (6), 1642-1667.
6. Yang, C.; Suo, Z., Hydrogel ionotronics. *Nature Reviews Materials* **2018,** *3* (6), 125.
7. Wang, Y.; Wang, Z.; Su, Z.; Cai, S., Stretchable and transparent ionic diode and logic gates. *Extreme Mechanics Letters* **2019,** *28*, 81-86.
8. Li, J.; Celiz, A.; Yang, J.; Yang, Q.; Wamala, I.; Whyte, W.; Seo, B.; Vasilyev, N.; Vlassak, J.; Suo, Z., Tough adhesives for diverse wet surfaces. *Science* **2017,** *357* (6349), 378-381.
9. Yuk, H.; Varela, C. E.; Nabzdyk, C. S.; Mao, X.; Padera, R. F.; Roche, E. T.; Zhao, X., Dry double-sided tape for adhesion of wet tissues and devices. *Nature* **2019,** *575* (7781), 169-174.
10. Yang, H.; Li, C.; Tang, J.; Suo, Z., Strong and degradable adhesion of hydrogels. *ACS Applied Bio Materials* **2019,** *2* (5), 1781-1786.
11. Li, J.; Mooney, D. J., Designing hydrogels for controlled drug delivery. *Nature Reviews Materials* **2016,** *1* (12), 1-17.
12. Flory, P. J., *Principles of polymer chemistry*. Cornell University Press: 1953.
13. Treloar, L. R. G., *The physics of rubber elasticity*. Oxford University Press, USA: 1975.
14. Di Lorenzo, F.; Seiffert, S., Nanostructural heterogeneity in polymer networks and gels. *Polymer Chemistry* **2015,** *6* (31), 5515-5528.
15. Seiffert, S., Origin of nanostructural inhomogeneity in polymer-network gels. *Polymer Chemistry* **2017,** *8* (31), 4472-4487.
16. Seiffert, S., Scattering perspectives on nanostructural inhomogeneity in polymer network gels. *Progress in Polymer Science* **2017,** *66*, 1-21.
17. Kizilay, M. Y.; Okay, O., Effect of swelling on spatial inhomogeneity in poly (acrylamide) gels formed at various monomer concentrations. *Polymer* **2004,** *45* (8), 2567-2576.
18. Sakai, T., Experimental verification of homogeneity in polymer gels. *Polymer Journal* **2014,** *46* (9), 517-523.
19. Gundogan, N.; Okay, O.; Oppermann, W., Swelling, Elasticity and Spatial Inhomogeneity of Poly (N, N‐dimethylacrylamide) Hydrogels Formed at Various Polymer Concentrations. *Macromolecular Chemistry and Physics* **2004,** *205* (6), 814-823.
20. Zhong, M.; Wang, R.; Kawamoto, K.; Olsen, B. D.; Johnson, J. A., Quantifying the impact of molecular defects on polymer network elasticity. *Science* **2016,** *353* (6305), 1264-1268.
21. Yang, C.; Yin, T.; Suo, Z., Polyacrylamide hydrogels. I. Network imperfection. *Journal of the Mechanics and Physics of Solids* **2019,** *131*, 43-55.
22. Lin, S.; Zhao, X., Fracture of polymer networks with diverse topological defects. *Physical Review E* **2020,** *102* (5), 052503.
23. Arvanitidou, E.; Hoagland, D., Chain-length dependence of the electrophoretic mobility in random gels. *Physical review letters* **1991,** *67* (11), 1464.
24. Rubinstein, M.; Colby, R. H., *Polymer physics*. Oxford university press New York: 2003; Vol. 23.
25. Shibayama, M.; Shirotani, Y.; Hirose, H.; Nomura, S., Simple scaling rules on swollen and shrunken polymer gels. *Macromolecules* **1997,** *30* (23), 7307-7312.

26. Langley, N. R.; Polmanteer, K. E., Relation of elastic modulus to crosslink and entanglement concentrations in rubber networks. *Journal of Polymer Science: Polymer Physics Edition* **1974,** *12* (6), 1023-1034.
27. Li, X.; Cui, K.; Kurokawa, T.; Ye, Y. N.; Sun, T. L.; Yu, C.; Creton, C.; Gong, J. P., Effect of mesoscale phase contrast on fatigue-delaying behavior of self-healing hydrogels. *Science Advances* **2021,** *7* (16), eabe8210.
28. Norioka, C.; Inamoto, Y.; Hajime, C.; Kawamura, A.; Miyata, T., A universal method to easily design tough and stretchable hydrogels. *NPG Asia Materials* **2021,** *13* (1), 1-10.
29. Furukawa, H.; Horie, K.; Nozaki, R.; Okada, M., Swelling-induced modulation of static and dynamic fluctuations in polyacrylamide gels observed by scanning microscopic light scattering. *Physical Review E* **2003,** *68* (3), 031406.
30. Kizilay, M. Y.; Okay, O., Effect of initial monomer concentration on spatial inhomogeneity in poly (acrylamide) gels. *Macromolecules* **2003,** *36* (18), 6856-6862.
31. Hasa, J.; Janáček, J. In *Effect of diluent content during polymerization on equilibrium deformational behavior and structural parameters of polymer network*, Journal of Polymer Science Part C: Polymer Symposia, Wiley Online Library: 1967; pp 317-328.
32. Orakdogen, N.; Okay, O., Effect of initial monomer concentration on the equilibrium swelling and elasticity of hydrogels. *European polymer journal* **2006,** *42* (4), 955-960.
33. Baker, J. P.; Hong, L. H.; Blanch, H. W.; Prausnitz, J. M., Effect of initial total monomer concentration on the swelling behavior of cationic acrylamide-based hydrogels. *Macromolecules* **1994,** *27* (6), 1446-1454.
34. Baselga, J.; Hernandez-Fuentes, I.; Pierola, I.; Llorente, M., Elastic properties of highly crosslinked polyacrylamide gels. *Macromolecules* **1987,** *20* (12), 3060-3065.
35. Dubrovskii, S. A.; Rakova, G. V., Elastic and osmotic behavior and network imperfections of nonionic and weakly ionized acrylamide-based hydrogels. *Macromolecules* **1997,** *30* (24), 7478-7486.
36. Orakdogen, N.; Okay, O., Correlation between crosslinking efficiency and spatial inhomogeneity in poly (acrylamide) hydrogels. *Polymer Bulletin* **2006,** *57* (5), 631-641.
37. Hu, Y.; Suo, Z., Viscoelasticity and poroelasticity in elastomeric gels. *Acta Mechanica Solida Sinica* **2012,** *25* (5), 441-458.
38. Kalcioglu, Z. I.; Mahmoodian, R.; Hu, Y.; Suo, Z.; Van Vliet, K. J., From macro-to microscale poroelastic characterization of polymeric hydrogels via indentation. *Soft Matter* **2012,** *8* (12), 3393-3398.
39. Dušek, K.; Galina, H.; Mikeš, J., Features of network formation in the chain crosslinking (co) polymerization. *Polymer Bulletin* **1980,** *3* (1-2), 19-25.
40. Baselga, J.; Llorente, M.; Nieto, J.; Hernández-Fuentes, I.; Piérola, I., Polyacrylamide networks. Sequence distribution of crosslinker. *European polymer journal* **1988,** *24* (2), 161-165.
41. Kizilay, M. Y.; Okay, O., Effect of hydrolysis on spatial inhomogeneity in poly (acrylamide) gels of various crosslink densities. *Polymer* **2003,** *44* (18), 5239-5250.
42. Baselga, J.; Llorente, M.; Hernandez-Fuentes, I.; Pierola, I., Polyacrylamide gels. Process of network formation. *European polymer journal* **1989,** *25* (5), 477-480.
43. Naghash, H. J.; Okay, O., Formation and structure of polyacrylamide gels. *Journal of applied polymer science* **1996,** *60* (7), 971-979.
44. Okay, O., Macroporous copolymer networks. *Progress in polymer science* **2000,** *25* (6), 711-779.

45. Okay, O.; Kurz, M.; Lutz, K.; Funke, W., Cyclization and reduced pendant vinyl group reactivity during the free-radical crosslinking polymerization of 1, 4-divinylbenzene. *Macromolecules* **1995,** *28* (8), 2728-2737.
46. Li, Z.; Liu, Z.; Ng, T. Y.; Sharma, P., The effect of water content on the elastic modulus and fracture energy of hydrogel. *Extreme Mechanics Letters* **2020,** *35*, 100617.
47. Bromberg, L.; Grosberg, A. Y.; Matsuo, E. S.; Suzuki, Y.; Tanaka, T., Dependency of swelling on the length of subchain in poly (N, N-dimethylacrylamide)-based gels. *The Journal of chemical physics* **1997,** *106* (7), 2906-2910.
48. Furukawa, H., Effect of varying preparing-concentration on the equilibrium swelling of polyacrylamide gels. *Journal of Molecular Structure* **2000,** *554* (1), 11-19.
49. Okay, O., Kinetic modelling of network formation and properties in free-radical crosslinking copolymerization. *Polymer* **1994,** *35* (4), 796-807.
50. Tanc, B.; Orakdogen, N., Influence of gel preparation concentration on statistical mechanics of poly (dialkylaminoethyl methacrylate) gels on the basis of scaling concept: Toward tunable elasticity and thermomechanical parameters. *Journal of Applied Polymer Science* **2020,** *137* (6), 48350.
51. Sakai, T., *Physics of Polymer Gels*. John Wiley & Sons: 2020.
52. Thomas, A., Rupture of rubber. V. Cut growth in natural rubber vulcanizates. *Journal of Polymer Science* **1958,** *31* (123), 467-480.
53. Lake, G.; Thomas, A., The strength of highly elastic materials. *Proceedings of the Royal Society of London. Series A. Mathematical and Physical Sciences* **1967,** *300* (1460), 108-119.
54. Nie, J.; Du, B.; Oppermann, W., Influence of formation conditions on spatial inhomogeneities in poly (N-isopropylacrylamide) hydrogels. *Macromolecules* **2004,** *37* (17), 6558-6564.
55. Shibayama, M.; Shirotani, Y.; Shiwa, Y., Static inhomogeneities and dynamics of swollen and reactor-batch polymer gels. *The Journal of Chemical Physics* **2000,** *112* (1), 442-449.
56. He, Q.; Wang, Z.; Yan, Y.; Zheng, J.; Cai, S., Polymer nanofiber reinforced double network gel composite: Strong, tough and transparent. *Extreme Mechanics Letters* **2016,** *9*, 165-170.
57. Li, J.; Illeperuma, W. R.; Suo, Z.; Vlassak, J. J., Hybrid hydrogels with extremely high stiffness and toughness. *ACS Macro Letters* **2014,** *3* (6), 520-523.
58. Wang, Z.; Xiang, C.; Yao, X.; Le Floch, P.; Mendez, J.; Suo, Z., Stretchable materials of high toughness and low hysteresis. *Proceedings of the National Academy of Sciences* **2019,** *116* (13), 5967-5972.
59. Long, R.; Hui, C.-Y.; Gong, J. P.; Bouchbinder, E., The fracture of highly deformable soft materials: A tale of two length scales. *Annual Review of Condensed Matter Physics* **2020,** *12*.
60. Chen, C.; Wang, Z.; Suo, Z., Flaw sensitivity of highly stretchable materials. *Extreme Mechanics Letters* **2017,** *10*, 50-57.
61. Akagi, Y.; Sakurai, H.; Gong, J. P.; Chung, U.-i.; Sakai, T., Fracture energy of polymer gels with controlled network structures. *The Journal of chemical physics* **2013,** *139* (14), 144905.
62. Li, C.; Yang, H.; Suo, Z.; Tang, J., Fatigue-resistant elastomers. *Journal of the Mechanics and Physics of Solids* **2020,** *134*, 103751.
63. Li, X.; Cui, K.; Sun, T. L.; Meng, L.; Yu, C.; Li, L.; Creton, C.; Kurokawa, T.; Gong, J. P., Mesoscale bicontinuous networks in self-healing hydrogels delay fatigue fracture. *Proceedings of the National Academy of Sciences* **2020,** *117* (14), 7606-7612.

64. Nakajima, T.; Furukawa, H.; Tanaka, Y.; Kurokawa, T.; Gong, J. P., Effect of void structure on the toughness of double network hydrogels. *Journal of Polymer Science Part B: Polymer Physics* **2011,** *49* (17), 1246-1254.
65. Yamaguchi, T.; Onoue, Y.; Sawae, Y., Topology and Toughening of Sparse Elastic Networks. *Physical Review Letters* **2020,** *124* (6), 068002.